Superlinear urban scaling by functional organization: A metabolic interpretation of sectoral water consumption

Likwan Cheng ⬤*

Physical Science Department, City Colleges of Chicago-Harold Washington College, Chicago, Illinois 60601, USA

Prevailing view asserts that the disproportionately greater productivities of larger cities, or superlinear urban scaling, are the result of human interactions channeled by urban networks. But this view was established by considering the spatial organization of urban infrastructure and social networks—the urban "arteries" effects—but neglecting the functional organization of urban production and consumption entities—the urban "organs" effects. Here, adopting a metabolic view and using water consumption as a proxy for metabolism, we empirically quantify the scaling of entity number, size, and metabolic rate for the functionally specific urban residential, commercial, public or institutional, and industrial sectors. Sectoral urban metabolic scaling is highlighted by a disproportionate coordination between residential and enterprise metabolic rates, attributable to the functional mechanisms of mutualism, specialization, and entity size effect. The resultant whole-city metabolic scaling exhibits a constant superlinear exponent for water-abundant regions in numerical agreement with superlinear urban productivity, with varying exponent deviations for water-deficient regions explainable as adaptations to climate-driven resource constraints. These results present a functional organizational, non-social-network explanation of superlinear urban scaling.

I. BACKGROUND

What gives rise to the disproportionately greater productivities of larger cities? Is it innovation and creativity unique to humans alone? Or is it also an evolved organizational optimality intrinsic to cities and organisms alike? An expansive and integrative understanding in the origins of urban scaling will help provide a complex systems foundation for developing effective policies for all aspects of urban sustainability [1]. This level of understanding requires unveiling the multilevel, multisectoral relations in the complex urban system [2]. Urban production and consumption can be conceived as metabolism, which scales nonlinearly with city size [3]. Influenced by precedences in metabolic scaling in living organisms, interpretations of urban metabolic scaling have so far largely embraced the concept of networks.

A. Transport-network model of organism metabolic scaling (sublinear)

In organisms, whole-organism metabolic rate is sublinearly scaled with organism mass, a phenomenon known as allometric scaling and is explained by energy allometry in the organism's optimal resource transport networks [3]. Cities are like organisms in two important ways in the transport network. The first is evolution. Cities evolve optimal infrastructural transport networks, such as roads [4] and water mains [5]. As a city grows, its infrastructure networks undergo dynamical continual and incremental renewals, tracing out in time a "common evolutionary track" on a graph containing cities at all stages of growth and obeying the scaling law relating infrastructure quantities and city size that signifies the optimality [6]. The second is efficiency. For example, the water supply system of a city is likened to "our own circulatory system" [3], differing only in hydraulic details: three-dimensional pressurized laminar flows of blood from the human heart versus two-dimensional pressurized turbulent flows of drinking water from the city water treatment plant. In similar ways, the bulk transports of blood in organism networks [7] and of water in urban networks [5] both exhibit sublinear (allometric) energy scaling with organism or city size, explainable by their respective hydraulic mechanisms.

B. Social-network model of urban metabolic scaling (superlinear)

But cities and organisms differ in one significant way. Whole-organism metabolism is sublinearly scaled with organism mass and is explainable by the energy allometry in organism transport networks; whole-city productivity is superlinearly scaled with city population and is not simply explainable by the energy allometry in urban transport networks [3]. This distinction has led to the speculation that superlinear urban scaling—the disproportionate increase in urban productivity with city size as measured by population—is a unique attribute of human settlements. The search for explanations has naturally been focused on the role of humans. Individual travels of humans in urban networks modeled after electrical conduction show superlinear energy scaling with city size [4]. Social-network models posit that human interactions facilitated by urban networks explain superlinear urban

————
*lcheng6@ccc.edu

scaling, and find exponent agreements with the scaling of urban socioeconomic productivity with city size as measured by population [4,8–10], thus establishing the prevailing view that social-network-driven greater human creative outputs in larger cities explain superlinear urban scaling.

C. Urban metabolism: From city as ecosystem to city as organism

The conventional view of urban metabolism conceives the city in terms of the flows of metabolic resources—energy, materials, and human resources—as well as wastes [11,12]; this view captures the multiplicity of processes in the city as a complex ecosystem [13]. An alternative, mostly neglected view of urban metabolism conceives the city in terms of the consumption of metabolic resources; this view captures the evolved organization of the city as an integral organism. It is the latter view, city as an organism, that provides the needed grounds for exploring the city as a complex, but organized system evolved to serve the functions of production and consumption. Overlooked for explaining urban metabolism [14], the organism view found application in explaining metabolisms in the river basin, helping establish organizational principles for the runoff [15] and transpiration [16] functions of the basin by considering "each nested subbasin as an organism" and addressing the "intraspecies scaling behavior" among a system of subbasins as reflecting the optimal functions of the whole basin [16].

Thus, the organism view of the city implies two levels of evolved organization. The first level of organization is an infrastructural organization within the city, which itself comprises two types. So far better recognized is the spatial organization, the hierarchical ordering of urban networks for efficient resource transports and human interactions. These roadways, water mains, sanitary canals, etc., are the equivalents of arteries and capillaries in an organism. So far mostly neglected is the functional organization, the mutual coordination among urban metabolic entities for efficient production and consumption. These factories, businesses, and schools, etc., in the enterprise sectors and households in the residential sector are the equivalents of major organs and ordinary tissues in an organism, respectively. The city is a (organismic) system of (organ and tissue) systems, with the coupling between enterprises (organs) and residents (tissues) reflecting the optimal function of the city (organism) as an overall system.

The second level of organization is a community organization among cities and communities. Larger cities supply metabolic products to smaller communities, such as treated drinking water [17]; in return, distant communities supply raw resources to large cities, such as human resources [18]. These symbiotic relations [19] systematically link the developments of central cities and distant lands [20], fostering an optimal regional community structure of cities and communities recognizable from the characteristic skewed size-abundance distribution of cities by population [21] or resource consumption [22]. The region is a (ecological) system of (organismic) systems, with the abundance of cities (organisms) by size reflecting the optimal function of the region (ecosystem) as an overall system.

D. Urban metabolic scaling: From networks to "organ"-ization

From the organism view of urban metabolism, social networks may not provide a complete explanation of superlinear urban scaling, because humans are not the only agents of urban metabolism and networks are not the only manifest of urban optimization. First, social-network models account for only the spatial organization of urban networks and its effects on human interactions, but they neglect the functional organization of urban metabolic entities and its effects on production and consumption. Second, the urban spatial network facilitates social interactions mainly within the city, but it "says little...about the 'system of cities' " [23] or the metabolic interactions among them. Although a more recent work has explored exogenous contributions to superlinear urban scaling, it has been restricted to the human factor of demographic differences [18].

How do urban "organs" and "tissues" functionally organize? Does this organization entail novel origins of whole-city metabolic scaling? These questions have remained unanswered because previous explorations of urban scaling have focused on spatial organization at the whole-city level [4,8–10,24–27] but neglected functional organization at the urban-sector level.

In this paper, we present a functional organizational interpretation of superlinear urban scaling. We conceptualize and apply the empirical analytical method of sectoral urban metabolic scaling (SUMS). With this method and based on the consumption of water as a resource, we deconstruct [28] whole-city scaling into scaling in the comprising, functionally specific urban sectors. We show that a metabolic interpretation of functional organization at the urban-sector level presents a numerically agreeable, non-social-network explanation of superlinear urban scaling at the whole-city level, with the additional ability of explaining scaling deviation as adaptation to regional resource constraints.

II. METHODS

Water is a common basic resource; the consumption or transport of water (or, more generally, any nutrient-carrying aqueous solution) has been used to measure metabolic scaling in many types of evolved complex systems, including living organisms [7], coastal estuary ecosystems [29], and the runoff [15] and transpiration [16] systems in river basins. Water metabolism is also the most studied process in conventional urban metabolism [14]. Following precedences, we use the consumption of water as a resource to measure urban metabolism. Beneficially, the water resource provides a relatively transport-insensitive measure of urban metabolism compared to energy resources [4,5] and a relatively demography-insensitive measure compared to human resources [18].

Resource abundance impacts metabolism. Since water abundance (along with temperature) defines climate conditions, we use climate zones as indicators of regional water abundance. Köppen classification of continental climates divides the midlatitude into humid and dry (arid or semiarid) climate zones [30]. We consider water-abundant regions (humid climate zones) as locations ideal for metabolic

optimization and treat water-deficient regions (dry climate zones) as locations likely to exhibit adaptive divergence from optimization.

For sectoral water consumption, we assembled 16 years of census data (2005–2020, where available) for cities in the water-abundant US states (regions) of Wisconsin (WI) and Pennsylvania (PA) in humid climate zones and cities in the water-deficient states of Utah (UT) and California (CA) in extensively dry and partially dry climate zones, respectively [31–34]. For whole-city consumption, we assembled additional data for cities in the water-abundant states of Illinois (IL), Missouri (MO), and New York (NY) in humid climate zones [35–37]. The inclusion of a state, cities within a state, year, or data type in this study is based solely on data availability. In each state, cities are defined as any census-designated places under local municipal governance, such as a city, village, borough, or community service district in a rural or an unincorporated area. Each city comprises four broadly defined functional sectors: residential, commercial, public or institutional, and industrial—the latter three to be collectively called enterprise sectors. Each sector comprises an ensemble of metabolic units or entities, e.g., a household in the residential sector, a school in the institutional sector, or a factory in the industrial sector. Using a bottom-up approach [38], we characterize sectoral organization by quantifying the scaling of number, size, and metabolic rate (water consumption) with city size. For a city, the number of metabolic entities N_i refers to the number of water customers in sector i. The size of a metabolic entity refers to the physical cross-sectional area of a customer's water meter, so that the sectoral cumulative size S_i is the summed cross-sectional area of all customer water meters in sector i. The metabolic rate of a metabolic entity refers to the annual metered water consumption of a customer, so that the sectoral cumulative metabolic rate M_i is the summed annual water consumption of all customers in sector i.

We develop a fractional scaling analysis; we consider the scaling of the sectoral variables N_i, S_i, and M_i with respect to the corresponding whole-city (all-sectors) variables N, S, and M, respectively, where, for example, $M = \sum_i M_i$. The whole-city quantity represents city size in this fractional context. We assume a power-law scaling relation. For example, for metabolic rate, we write

$$M_i = AM^b, \tag{1}$$

where A is the prefactor and b is the scaling exponent. By logarithmic transformation, we obtain

$$\log M_i = a + b \log M, \tag{2}$$

where $a = \log A$. Each coordinate data point $(x, y) = (\log M, \log M_i)$ represents a city and the ensemble data set $\{x, y\} = \{\log M, \log M_i\}$ represents a region of cities. In a least-square (LS) linear fit of Eq. (2), of the best-fit parameters a is the intercept and b (the scaling exponent) is the slope of the ensemble. (For notational simplicity, we omit the scripts for cities on the variables and the scripts for sectors on the parameters.)

Both whole-city and sectoral metabolic rates, M and M_i, respectively, show lognormal abundance distributions. With the logarithmic transformation, the lognormally distributed M

is converted to normally distributed $\log M$, where the mean of $\log M$ marks the median of M and the standard deviation (SD) of $\log M$ is an indicator of the skewness of M; likewise for M_i. In the LS formulation, the slope b is defined as [39]

$$b = R\frac{\sigma_i}{\sigma}, \tag{3}$$

where R is the correlation between $\log M$ and $\log M_i$, and σ and σ_i are the SDs of the normal distributions of $\log M$ and $\log M_i$, respectively. Slopes of $b < 1$, $b = 1$, and $b > 1$ correspond to sublinear (allometric), linear (proportional), and superlinear scaling of M_i with M, respectively.

Equation (3) connects sectoral scaling and sectoral size abundance distribution. The fractionally dominant residential distribution is necessarily strongly associated with the whole-city distribution in both the rank order of cities and SD, resulting in $R \lesssim 1$ and $\sigma_i/\sigma \lesssim 1$; the fractionally nondominant enterprise sectors are freer to have larger sectoral SDs through tradeoffs among themselves, which necessarily entails rank shifts among cities in sectoral metabolism, resulting in $\sigma_i/\sigma > 1$ and $R < 1$.

Now that the correlation R has a systematic sectoral dependence, we introduce a new ensemble parameter, dispersion s, to capture this physical (rather than random statistical) behavior, defined as the SD of the fit residuals $\{y - \hat{y}\}$ to Eq. (2), where $\hat{y}$ is the LS model-predicted value of $\log M_i$, or

$$s = \text{SD}(\{y - \hat{y}\}). \tag{4}$$

For metabolism, the set of parameters (a, b, s) of intercept, slope, and dispersion describe the ensemble characteristics of sectoral metabolic rate, growth of sectoral metabolic rate with city size (defined by whole-city metabolic rate), and the variability of sectoral metabolic rate, respectively.

III. RESULTS

A. Overall observations

SUMS results show that the two key features of urban optimality known to manifest at the whole-city level (nonlinear scaling [3] and skewed abundance distribution [21]) both also manifest at the urban-sector level, but with sectorally dependent parameters that reflect function specificity. SUMS results are shown as yearly parameters in time series (2005–2020, where available) in Fig. 1, as averaged parameters across years in Table I, as one-year representative scaling data and fits in Fig. 2, and as one-year representative abundance distribution data and fits in Fig. 3. The one-year representative data are from 2018, where available, the most recent complete annual data sets at the time of study. Complete yearly scaling data and fits are shown in Figs. S1– S20 [40].

At the sectoral level, for each type of enterprise, the number of enterprise entities (urban organs) grows more slower than that of all metabolic entities of the city [Fig. 1(a), 6–8] while the cumulative physical size of the enterprise entities grows less slower than that of all metabolic entities of the city [Fig. 1(b), 6–8], so that the per-entity physical size of the enterprise entities grows distinctly faster than that of all metabolic entities of the city [$b > 0$; Fig. 1(c), 6–8]. Conversely, the number of residential entities (urban tissues) grows marginally faster than that of all entities [Fig. 1(a),
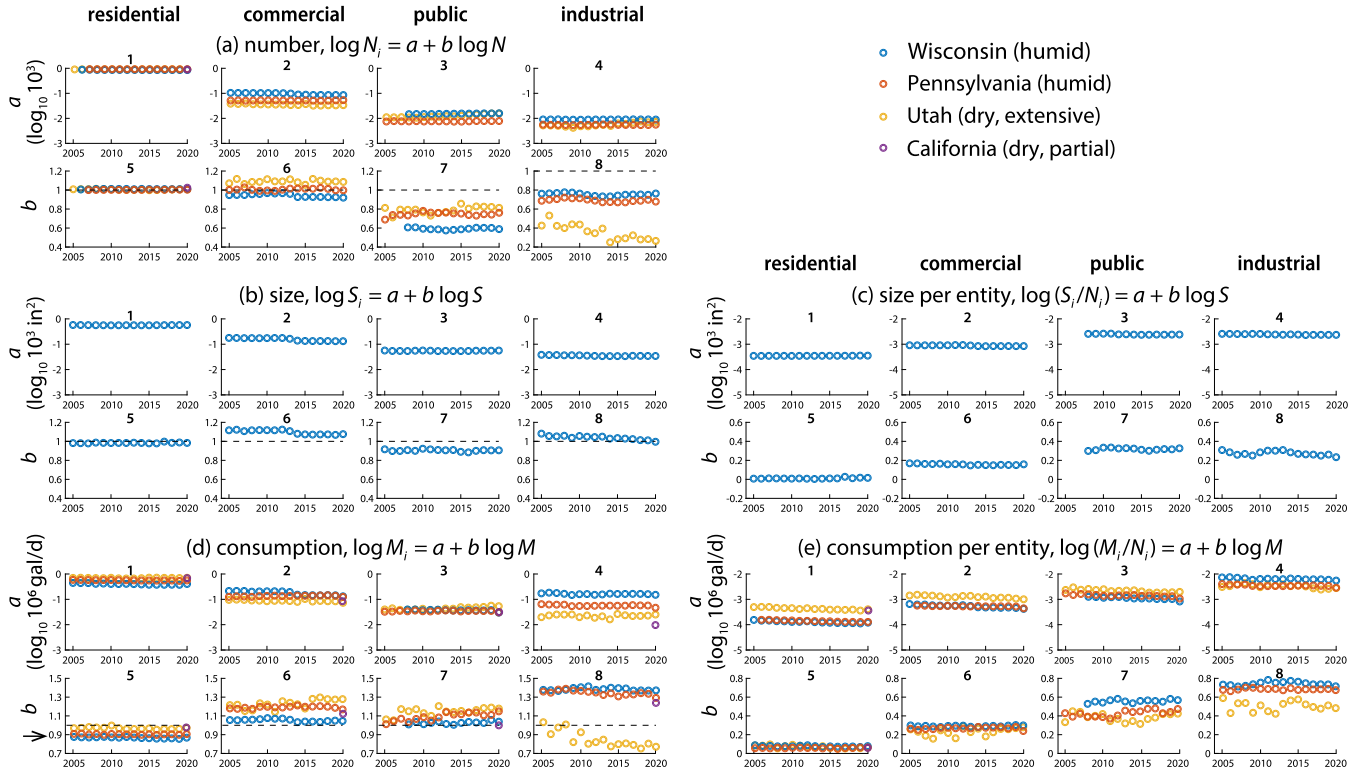
FIG. 1. Sectoral urban metabolic scaling. Sixteen-year (2005–2020) time series of best-fit slopes b and intercepts a for sectoral vs. whole-city (fractional) scaling of (a) entity number, (b) size, (c) size per entity, (d) water consumption (as metabolic rate), and (e) water consumption per entity for cities in WI, PA (both humid), UT (extensively dry), and CA (partially dry). Superlinear urban scaling of consumption with population results from the inverse of the sublinear residential fractional scaling [(d), panel 5, indicated by the arrow], given that residential consumption is proportional to residential population under water-abundant (humid) conditions.

5] while the cumulative physical size of the residential entities grows marginally more slowly than that of all entities [Fig. 1(b), 5], so that the per-entity physical size of the residential entities grows little differently than that of all entities [$b \simeq 0$; Fig. 1(c), 5].

At the per-entity level, the physical size of entities [Fig. 1(c), 1–4] and the rates of growth of physical size [Fig. 1(c), 5–8] follow the same trend ordered by sector. The systematic trend of "large get larger" in per-entity physical size [Fig. 1(c)] is counterbalanced by the

TABLE I. Fractional scaling parameters by sector in number of entities, size, and water consumption (as metabolic rate).

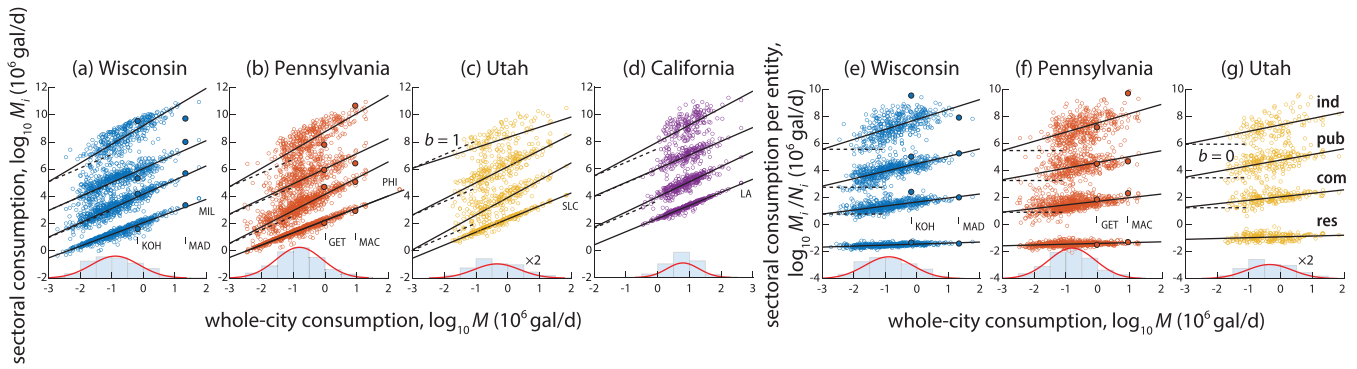| Sector	Cities		Number			Size			Water consumption				
		n	exponent b	prefactor A	disp. s	exponent b	prefactor A (in^2)	disp. s	exponent b	prefactor A (10^{6}gal/d)	disp. s	correlation R^2	distribution σ_i/σ
Residential	WI	570	1.01 (0.01)	858 (6)	0.04	0.98 (0.02)	564 (16)	0.12	0.87 (0.02)	0.40 (0.02)	0.19	0.92	0.87 (0.02)
	PA	633	1.00 (0.01)	915 (6)	0.03				0.90 (0.02)	0.56 (0.02)	0.16	0.94	0.92 (0.01)
	UT	181	1.01 (0.01)	913 (11)	0.04				0.97 (0.03)	0.69 (0.04)	0.14	0.96	0.97 (0.04)
	CA	358	1.01 (0.03)	846 (87)	0.05				0.97 (0.02)	0.68 (0.03)	0.10	0.96	1.01 (0.01)
Commercial	WI	563	0.95 (0.04)	95 (4)	0.23	1.09 (0.03)	155 (9)	0.24	1.05 (0.04)	0.17 (0.02)	0.32	0.87	1.11 (0.01)
	PA	621	1.01 (0.05)	52 (4)	0.37				1.19 (0.05)	0.13 (0.02)	0.43	0.80	1.36 (0.01)
	UT	157	1.09 (0.11)	35 (6)	0.45				1.23 (0.13)	0.09 (0.02)	0.56	0.71	1.45 (0.05)
	CA	339							1.11 (0.07)	0.09 (0.01)	0.30	0.76	1.23 (0.01)
Public	WI	531	0.59 (0.04)	15 (1)	0.27	0.90 (0.05)	55 (5)	0.38	1.03 (0.06)	0.04 (0.01)	0.51	0.68	1.07 (0.02)
	PA	380	0.75 (0.07)	8 (1)	0.44				1.09 (0.09)	0.03 (0.01)	0.59	0.59	1.30 (0.01)
	UT	131	0.79 (0.10)	12 (2)	0.35				1.14 (0.14)	0.04 (0.01)	0.55	0.66	1.40 (0.05)
	CA	195							1.01 (0.11)	0.03 (0.01)	0.38	0.63	1.26 (0.02)
Industrial	WI	392	0.76 (0.06)	9 (1)	0.36	1.04 (0.08)	35 (5)	0.49	1.38 (0.09)	0.16 (0.04)	0.66	0.68	1.49 (0.03)
	PA	391	0.69 (0.08)	6 (1)	0.44				1.34 (0.12)	0.06 (0.01)	0.72	0.59	1.68 (0.02)
	UT	80	0.36 (0.18)	6 (2)	0.50				0.85 (0.26)	0.02 (0.01)	0.75	0.28	1.36 (0.05)
	CA	197							1.25 (0.23)	0.01 (0.01)	0.74	0.36	1.85 (0.03)

FIG. 2. Data (colored circles, each representing a city) and fits (solid black lines) for the scaling of (a)–(d) sectoral cumulative water consumption and (e)–(g) sectoral per-entity water consumption with whole-city water consumption for cities in WI, PA (both humid), UT (extensively dry), and CA (partially dry). Histograms show log-transformed distributions of whole-city consumptions with log-space normal distribution fits (red curves). Highlighted data points indicate the functionally specialized cities of Madison (MAD; public), Kohler (KOH; industrial), Macungie (MAC; industrial), and Gettysburg (GET; commercial). For clarity, the plots for the residential, commercial, public, and industrial sectors are shifted on the vertical axis by 2.5, 5, 7.5, and 10, respectively. The largest city in each state is labeled: Milwaukee (MIL), Philadelphia (PHI), Salt Lake City (SLC), and Los Angeles (LA).

systematic trend of "large get fewer" in entity number [Fig. 1(a), 1–4]. This counterbalance between number and size lays the foundation for the organization in consumption (metabolism), which shows an increasing trend in per-entity metabolic rate [Fig. 1(e), 1–4] but a (mostly) decreasing trend in cumulative metabolic rate [Fig. 1(d), 1–4] across the sectors as ordered by increasing per-entity size. Sectoral scaling parameters in consumption (intercept a, dispersion s, and slope b) can be explained by a metabolic interpretation based on the evolution principles of mutualism, specialization, and size effect (efficiency), respectively, as described below. Deviations in the parameters are explainable as climate-driven adaptive divergence, as described in Sec. IV B.

B. Metabolic interpretation of scaling parameters

1. Intercept

Sectoral intercepts reflect functional mutualism. The sectoral metabolic rates, measured by the intercept $a = \log A$, are disproportionately coupled among the sectors. In the water-abundant regions, the residential sector has a large [Fig. 1(d), 1] but slowly decreasing metabolic rate with city

size ($A_{\rm res} = 0.40 \pm 0.02$ for WI, $A_{\rm res} = 0.56 \pm 0.02$ for PA; Table I) and the enterprise sectors have smaller [Fig. 1(d), 2–4] but overall faster increasing metabolic rates with city size (e.g., $A_{\rm ind} = 0.16 \pm 0.04$ for WI, $A_{\rm ind} = 0.06 \pm 0.01$ for PA; Table I). This coupling reflects a residential-enterprise mutualism in metabolism. The mutualism argument draws its analogy from the ecosystem view that functions are a determinant of metabolic scaling [41]. In the urban setting, enterprises depend on residents as labor force and consumers whereas residents depend on enterprises for employment and resources to sustain livelihood.

Sectoral coupling provides stability to urban metabolism, as the endogenous residential sector's large entity number [Fig. 1(a), 1] and dominant metabolic rate [Fig. 1(d), 1] help buffer impacts from the faster-growing [Fig. 1(d), 6–8], partially exogenously influenced enterprise sectors, making changes incremental and adaptable. At the same time, sectoral coupling allows for flexibility for adaptation. For example, the increased pace of life with city size [42] can be interpreted as a residential adaptation to superlinearly scaled industrial metabolism, and the concurrent increase in residential water consumption but decrease in industrial water consumption in
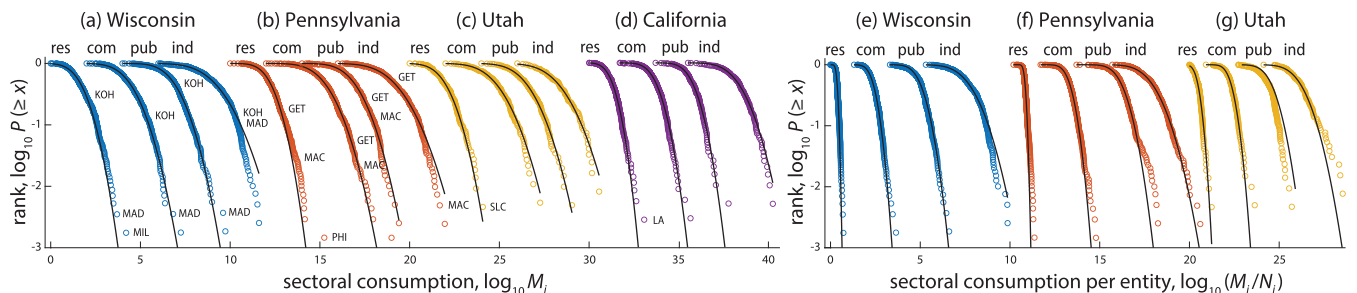

FIG. 3. Rank-size distributions of cities in (a)–(d) sectoral cumulative water consumption and (e)–(g) sectoral per-entity water consumption shown as the ranked probability (y axis) of finding consumption sizes equal to or greater than a given consumption size (x axis) for cities in WI, PA, UT, and CA. Solid lines are lognormal distribution fits (average $R^2 = 0.99$; two-sample Komogorov-Smirnov test for lognormalcy, average $p = 0.92$). Rank locations of the specialized cities and the largest city in each state (see Fig. 2 caption) are indicated. For clarity, the plots are relatively shifted on the horizontal axis.

dry climates can be interpreted as an adaptation to resource constraint (Sec. IV B).

2. Dispersion

Sectoral dispersions reflect functional specialization. The dispersions of metabolic rates, measured by the residual SD s, show a sectoral dependence, with a small dispersion for the residential sector ($s_{res} = 0.19$ for WI, $s_{res} = 0.16$ for PA; Table I) and larger dispersions for the enterprise sectors (e.g., $s_{ind} = 0.66$ for WI, $s_{ind} = 0.72$ for PA; Table I). As cities seek growth through exogenous demands, the needs for supply-demand balance [43] and for residential-enterprise coupling must be met. This requires the metabolic increases in one enterprise sector to be offset by decreases in other enterprise sectors, resulting in increased individual residuals that collectively give the larger dispersions for enterprise sectors.

For example, the city of Madison, specializing in governmental and higher education functions, has an above-prediction public metabolic rate but a below-prediction industrial metabolic rate; Macungie, specializing in truck manufacturing, and Kohler, specializing in plumbing appliances manufacturing, both have above-prediction industrial metabolic rates but below-prediction public metabolic rates; Gettysburg, specializing in historic landmarks preservation and tourism, has a below-prediction industrial metabolic rate but an above-prediction commercial metabolic rate. But all four cities have approximately as-predicted residential metabolic rates as the enterprise residuals are mutually offsetting (Fig. 2). While specialization rearranges industrial rank orders (Fig. 3) and reduces the correlation between industrial metabolic rates and the whole-city metabolic rates ($R^2 = 0.68$ for WI, $R^2 = 0.59$ for PA; Table I), the rank order of residential metabolic rates remains strongly correlated with that of the whole-city metabolic rates ($R^2 = 0.92$ for WI, $R^2 = 0.94$ for PA; Table I) because the residential rates dominate the whole-city rates [Fig. 1(d), 1]. The anchoring of whole-city metabolism by the endogenous residential metabolism helps ensure the stability of the city despite the partially exogenous causes of enterprise metabolisms.

Dispersion reflecting specialization conforms with the finding of complex systems physics that coordinated heterogeneity is favored over homogeneity for system stability [44] and with the principle of ecology that functional differentiation and complementarity among individuals (cities) promote stability in the population (the region) [45]. In sectoral metabolism, slope b is highly directly associated with dispersion s, having the Pearson correlation coefficient $\rho(b, s) = 0.86$, as expected in the analysis of Eq. (3). This association implicates a connection between enterprise superlinear productivity, especially industrial superlinear productivity [Fig. 1(d), 8], and exogenous demands, as productions in one city feed to consumptions in other cities. Therefore, enterprise metabolic dispersions account for transboundary metabolic interactions among a system of cities in a region (or, by extension, in a country or the globe).

3. Slope

Sectoral slopes reflect functional size effects. The growths of sectoral metabolic rates with city size, measured by the

slope b, are unequal among urban sectors, with the residential sector having a sublinear slope ($b_{res} = 0.87 \pm 0.02$ for WI, $b_{res} = 0.90 \pm 0.02$ for PA; Table I) and the enterprise sectors having superlinear slopes, most so for the industrial sector ($b_{ind} = 1.38 \pm 0.09$ for WI, $b_{ind} = 1.34 \pm 0.12$ for PA; Table I). Functional size effects are explainable by the supply side of metabolism. Larger cities evolve larger enterprise organs through the mechanisms of spatial concentration and temporal expansion; for example, the shopping center spatially brings together stores to increase sales and the factory implements temporal work shifts to expand production hours, respectively. These mechanisms lead to functional size effects at the entity level.

The correspondence in the sectorally ordered trend between per-entity physical sizes [Fig. 1(c)] and per-entity metabolic rates [Fig. 1(e)] traces size effects in entity-level metabolic rates to entity-level physical sizes. The correspondence in the sectorally ordered trend between per-entity metabolic exponents [Fig. 1(e), 5–8] and cumulative metabolic exponents [Fig. 1(d), 5–8] traces sectoral cumulative scaling to sectoral per-entity scaling. The contrasts between residential and enterprise sectors in per-entity metabolic scaling [Fig. 2(e)–2(g)] and in per-entity metabolic size abundance [Fig. 3(e)–3(g)] also indicate that functions of the enterprise organs, especially the industrial organs, are linked to entity-level size effects. Entity-level size effects associated with functional organization contrast whole city-level size effects associated with social interactions; they represent a distinct origin of urban scaling.

IV. DISCUSSION

A. Urban-organs model of urban metabolic scaling (superlinear)

We now use SUMS results to explain superlinear urban scaling, the disproportionate increase in urban productivity with city size as measured by population. First, urban water consumption is a proper proxy for urban production because the two scale similarly. Whole-city economic productivity exhibits superlinear scaling with city population, having empirical exponents in the range around 1.07–1.15. Examples from the literature include: urban gross domestic product in metropolitan statistical areas in the US ($b = 1.13 \pm 0.02$) [4], incomes in urban areas in the US ($b = 1.15$, $R^2 = 0.97$) [46], labor in metropolitan areas in Brazil ($b = 1.11 \pm 0.07$) [47], labor markets in Sweden ($b = 1.08 \pm 0.02$) [18], and urban product in more developed cities in China ($b = 1.11$, $R^2 = 0.72$) [27]. Whole-city water consumption (under water-abundant conditions) also exhibits superlinear scaling with city population, having empirical exponents in a similar range [26]. Cases presented in this study for the humid states are: $b = (1.06, 1.14)$ for WI, $b = (1.06, 1.10)$ for PA, $b = (1.05, 1.09)$ for IL, $b = (1.07, 1.13)$ for MO, and $b = (1.07, 1.13)$ for NY [Fig. 4(a)–4(e); Table II].

Second, superlinear scaling of whole-city water consumption with population can be explained by functional organization as revealed by SUMS. This organization is underpinned by the counterbalance between "large get larger" in entity size and "large get fewer" in entity number; it entails
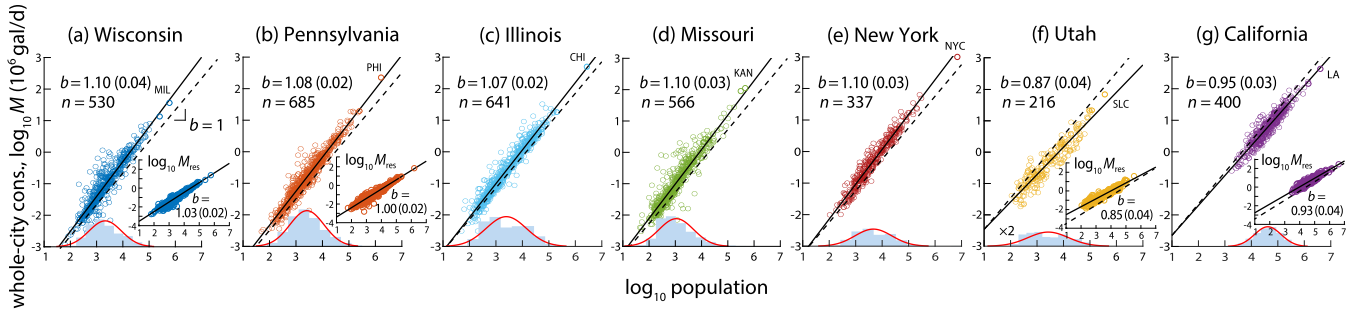
FIG. 4. Data (colored circles, each representing a city) and fits (solid black lines) for the scaling of whole-city water consumption with city population for cities in WI, PA, IL, MO, NY (all humid), UT (extensively dry), and CA (partially dry). Histograms show log-transformed distributions of city populations with log-space normal distribution fits (red curves). Dashed lines are references of linear scaling ($b = 1$). The largest city in each state is labeled: Milwaukee (MIL), Philadelphia (PHI), Chicago (CHI), Kansas City (KAN), New York City (NYC), Salt Lake City (SLC), and Los Angeles (LA). Insets show scaling of residential sectoral consumption with population (Fig. S21 [40]).

that, for the small size but large number of the residential entities, the residential metabolic rate will scale slightly sublinearly with the whole-city metabolic rate in fractional scaling [Fig. 1(d), 5, indicated by the arrow] or, conversely, the whole-city metabolic rate will scale slightly superlinearly with the residential metabolic rate. Additionally, residential water consumption is expected to scale linearly with residential population under water-abundant conditions, as verified by data for the humid states: $b = 1.03 \pm 0.02$ for WI and $b = 1.00 \pm 0.02$ for PA (Fig. 4(a), 4(b) insets; see Fig. S21 for details [40]). Substituting population for residential consumption, SUMS predicts that the whole-city metabolic rate will scale slightly superlinearly with city population; for the humid states: $b = (1.12, 1.18)$ for WI and $b = (1.08, 1.14)$ for PA, in approximate agreement with observations and correctly explaining superlinear urban scaling. The range of the exponent values itself has significance in the metabolic perspective, as too large a superlinearity would decouple residential-enterprise mutualism and destabilize the city whereas too small or an absence of a superlinearity would fail to account for exogenous interactions among cities. For the central role of urban enterprise entities in effecting the superlinear scaling, this model may be called the "urban-organs model".

B. Adaptive divergence in urban scaling

The scaling deviations for UT and CA can be explained as evolved adaptive divergence in response to climate-driven

TABLE II. Scaling of whole-city water consumption (as metabolic rate) with city population.

State	Cities n	Climate	Slope b	Intercept a ($\log_{10} 10^6$ gal/d)
Wisconsin	530	humid	1.10(0.04)	−4.71(0.13)
Pennsylvania	685	humid	1.08(0.02)	−4.49(0.08)
Illinois	641	humid	1.07(0.02)	−4.21(0.07)
Missouri	566	humid	1.10(0.03)	−4.31(0.11)
New York	337	humid	1.10(0.03)	−4.35(0.11)
California	400	dry, partial	0.95(0.03)	−3.60(0.16)
Utah	216	dry, extensive	0.87(0.04)	−3.34(0.15)

resource (water) constraints of varying degrees. For UT, the second driest state in the US situated mostly within semiarid and arid climate zones, the deviations are clearer. First, the residential consumption shows a higher per-entity value in fractional scaling [Fig. 1(e), 1] and a higher per-capita value and sublinear slope in scaling with population (Fig. 4(f) inset; Fig. S21 [40]), contrasting the lower per-entity and per-capita values and linear slope for the humid states. The higher consumption values concur with the region's high evapotranspiration rates [48], and the sublinear slope suggests that the scarcity of a resource has activated economies of scale in its consumption. Second, the industrial consumption has a lower intercept and a poorly correlated, sublinear slope [Fig. 1(d), 8], contrasting the superlinear slopes for the humid states. These related parametric deviations can be explained by considering Eq. (3), $b_i = R(\sigma_i/\sigma)$; here, the industrial sectoral metabolic distribution remains mostly intact [$\sigma_{ind}/\sigma = 1.36 \pm 0.05$; Fig. 3(c)], but its correlation with the whole-city metabolic distribution is diminished ($R^2 = 0.28$), suggesting the semiarid region's known large geographic heterogeneity in water resources [48] has disrupted the city size-based industrial metabolic rank order, losing the superlinearity in the fractional scaling of industrial entity number [Fig. 1(a), 8] and metabolic rate [$b_{ind} = 0.85 \pm 0.26$; Fig. 1(d), 8].

Although CA's highly varied climates also include semiarid and arid zones, the proportions are small compared to UT and the state's water deficiency is actively mitigated with some of the world's most prominent systems of transbasin diversion and conveyance (e.g., the Colorado River Aqueduct) [49]. Likely as a result, the scaling behaviors for CA fall between that for UT and the humid states. Like UT, CA's residential consumption also shows a higher per-entity value in fractional scaling [Fig. 1(e), 1] and a higher per-capita value and sublinear slope in scaling with population (Fig. 4(g) inset; Fig. S21 [40]); but like WI and PA, CA's industrial consumption shows a superlinear slope [Fig. 1(d), 8], with a low intercept [Fig. 1(d), 4] perhaps partly attributable to the state's less water-demanding, technology-focused industries. For the dry regions, $b = (0.83, 0.91)$ for UT and $b = (0.92, 0.96)$ for CA for whole-city water consumption with population; the varying extents of exponent deviation from the values under water-abundant conditions reflect the varying degrees of water

deficiency of the two regions, conforming with the interpretation of adaptive divergence.

In plants, water stress induces the tradeoff of seed production for tolerance, resulting in scaling deviations [50]; in cities, water stress induces the tradeoff of industrial production for residential living, also resulting in scaling deviations. Different levels of resource abundance activate different sets of metabolic functions [45]; in turn, "mixing different 'cocktails' of the components" [51] results in different exponents in whole-organism (whole-city) scaling. Since resource limitation impacts the scaling exponent [41,50], there is no single b [52]. Thus, the metabolic interpretation avails the rationale of adaptation to resource constraints to explain exponent deviations in urban scaling, which have often been observed but inadequately explained by existing scaling models [53].

C. Reconciling urban-organs model and social-network model

The urban-organs model of functional organization and the social-network model of human interactions represent physically distinct urban manifests but have numerically overlapping scaling exponents. The two models are conceived upon different origins of urban nonlinearity. In the social-network model, scaling arises from the spatial geometric order among urban network segments, from side streets to expressways, laid out in hierarchy as one city-level network; in the urban-organs model, scaling arises from the functional metabolic order among urban production and consumption entities, from households to factories, fostered by mutualism among a large number of individual entities. In the social-network view, a larger city produces more because its network is comprised of a disproportionate fraction of wider segments; in the urban organs view, a larger city produces more because its metabolism is driven by a disproportionate fraction of organs.

Urban productions strongly associated with enterprise operations (e.g., factory manufacturing) are better explained by the urban-organs model; urban productions strongly associated with social interactions (e.g., patent creation) are better explained by social-network models. The contrasting views of the city explored here as a complex system find historical precedence in urban cultural debates. Support for the social-network models has often been cited from the philosophical argument of the early 20th-century urban scholar Jane Jacobs, who recognized the city as a complex organism in which social interactions are a key to urban vitality [54]. Equally convincing support can be cited for the urban-organs model from the contrasting philosophical argument of another early 20th-century urban scholar, Daniel Burnham, who also viewed the city as a complex organism, but in light of civic organization, an urban ideal widely regarded by historians as the blueprint of modern American cities [55].

D. Reconciling urban-organs model and transport-network model

Given the optimal transport network present in both organisms and cities, why do organisms take advantage of it to reduce metabolic rates ($b < 1$ in whole-organism scaling) but cities take advantage of it to metabolize even more ($b > 1$ in whole-city scaling)? This may be explained by a difference in system boundary. Organisms are more self-contained systems and do not ordinarily export metabolic products directly into another organism, but cities are more connected and do export products to other cities.

Given the context, both organisms and cities may manifest organs effects. In birds, temperate birds evolved larger organs and higher metabolic rates than tropical birds in order to meet the external challenge of colder climates [56,57]; in cities, large cities evolved larger-sized enterprise entities [Fig. 1(c), 2–4] and higher metabolic rates [Fig. 1(e), 2–4] in order to meet the exogenous demands from smaller communities. For cities, metabolic optimization is done more for the whole region rather than for the individual city, as supported by the observed sectoral lognormal abundance distributions (Fig. 3). Regional optimization limits the number of enterprise entities to reduce construction and operational costs and preferentially places these entities in larger cities for economies of scale, including transport allometry [3]. These arguments are consistent with the observed increasing growths in organ sizes [Fig. 1(c), 6–8] and metabolic rates [Fig. 1(e), 6–8] but decreasing growths in organ numbers [Fig. 1(a), 6–8] with city size in fractional scaling that ultimately result in whole-city superlinear metabolic scaling with population.

V. CONCLUSION

Previous works relying on whole-city metabolic scaling without sectoral discretions have concluded that human interactions in spatial networks explain superlinear urban productivity. Now, based on sectoral metabolic scaling invoking neither spatial networks nor human interactions, we have shown that the functional organization among urban metabolic entities also explains superlinear urban productivity. Besides numerical agreement in the scaling exponent, the urban-organs model finds interpretive agreements with three key observable characteristics of the city: stability of the city (interpretable by residential-enterprise metabolic mutualism), functional specialization of the city (interpretable by enterprise metabolic dispersions), and adaptation of the city to resource constraints (interpretable by the divergence in scaling exponents). This metabolism-based, functional organizational interpretation of the city stands to complement the existing social-interaction interpretation of the city, helping bring about a more expansive and integrative view of urban scaling.

In particular, the sensitivity of the scaling parameters to climate-driven resource constraints suggests potential applicabilities of SUMS and its derivative urban organs model. Climate change is already driving the shifts of continental climate zones, causing expansions and degradations of dry climate zones [58]. The sublinearly scaled industrial metabolic rates observed for the semiarid state of UT, contrasting the superlinearly scaled ones observed for the humid states, suggest climate change could cause water stress-induced nonlinear negative responses in urban productivity, potentially compounding temperature increase-induced nonlinear negative responses in urban productivity already predicted [59]. Potential climate migration of urban industries, suggestive by the recently evolving, increasingly sublinearly scaled industrial

entity number for UT [Fig. 1(a), 8], could threaten to both decouple the residential-enterprise mutualism within the city and disrupt the regional industrial rank order among cities. As an analytical approach on urban metabolism, SUMS possesses function specificity, scale generality, and climate sensitivity. It may be used as a systems probe for predicting sector-specific responses in urban production and consumption to climate change in a regional system of cities and communities. As such, SUMS and the urban-organs model may contribute

to the timely scientific thrust of bringing complex systems approaches to applications in climate change and urban sustainability.

[1] National Academies of Sciences, Engineering, and Medicine, *Pathways to Urban Sustainability: Challenges and Opportunities for the United States* (The National Academies Press, Washington, DC, 2016)

[2] A. Ramaswami, A. G. Russell, P. J. Culligan, K. R. Sharma, and E. Kumar, Science **352**, 940 (2016).

[3] G. B. West, *Scale: The Universal Laws of Growth, Innovation, Sustainability, and the Pace of Life in Organisms, Cities, Economies, and Companies* (Penguin Press, New York, 2017).

[4] L. M. A. Bettencourt, Science **340**, 1438 (2013).

[5] L. Cheng and B. W. Karney, Phys. Rev. E **96**, 062317 (2017).

[6] L. Cheng and B. W. Karney, Phys. Rev. E **98**, 062323 (2018).

[7] G. B. West, J. H. Brown, and B. J. Enquist, Science **276**, 122 (1997).

[8] S. Arbesman, J. M. Kleinberg, and S. H. Strogatz, Phys. Rev. E **79**, 016115 (2009).

[9] W. Pan, G. Ghoshal, C. Krumme, M. Cebrian, and A. Pentland, Nature Commun. **4**, 1961 (2013).

[10] K. Yakubo, Y. Saijo, and D. Korošak, Phys. Rev. E **90**, 022803 (2014).

[11] C. Kennedy, S. Pincetl, and P. Bunje, Environ. Pollution **159**, 1965 (2011).

[12] Y. Zhang, Z. Yang, and X. Yu, Environ. Sci. Tech. **49**, 11247 (2015).

[13] N. Golubiewski, Ambio **41**, 751 (2012).

[14] J. P. Newell and J. J. Cousins, Prog. Hum. Geog. **39**, 702 (2015).

[15] A. Rinaldo, R. Rigon, J. R. Banavar, A. Maritan, and I. Rodriguez-Iturbe, Proc. Natl. Acad. Sci. USA **111**, 2417 (2014).

[16] I. Rodriguez-Iturbe, K. K. Caylor, and A. Rinaldo, Proc. Natl. Acad. Sci. USA **108**, 11751 (2011).

[17] L. Cheng, Water-Energy Nexus **4**, 1 (2021).

[18] M. Keuschnigg, S. Mutgan, and P. Hedström, Sci. Adv. **5**, eaav0042 (2019).

[19] UN Habitat, *World Cities Report 2020: The Values of Sustainable Urbanization* (UN Habitat, Nairobi, Kenya, 2020).

[20] K. C. Seto, A. Reenberg, C. G. Boone, M. Fragkias, D. Haase, T. Langanke, P. Marcotullio, D. K. Munroe, B. Olah, and D. Simon, Proc. Natl. Acad. Sci. USA **109**, 7687 (2012).

[21] M. Batty, *The New Science of Cities* (MIT Press, Cambridge, 2013).

[22] L. Cheng, Environ. Sci. Tech. **54**, 5071 (2020).

[23] M. Batty, Science **340**, 1418 (2013).

[24] V. C. Yang, A. V. Papachristos, and D. M. Abrams, Phys. Rev. E **100**, 032306 (2019).

[25] S. G. Ortman, A. H. F. Cabaniss, J. O. Sturm, and L. M. A. Bettencourt, Sci. Adv. **1**, e1400066 (2015).

[26] A. Ramaswami, D. Jiang, K. Tong, and J. Zhao, J. Ind. Ecol. **22**, 392 (2018).

[27] X. Liu and Z. Zou, PLoS One **15**, e0236593 (2020).

[28] E. Arcaute, E. Hatna, P. Ferguson, H. Youn, A. Johansson, and M. Batty, J. R. Soc. Interface. **12**, 20140745 (2015).

[29] N. J. Nidzieko, Proc. Natl. Acad. Sci. USA **115**, 6733 (2018).

[30] E. J. Tarbuck and F. K. Lutgens, *Earth Science*, 15th ed. (Pearson, Hoboken, 2017).

[31] Wisconsin Public Service Commission, Water Utility Data, Accessed: 2021.

[32] Pennsylvania Department of Environmental Protection, Water Reports, Accessed: 2021.

[33] Utah Department of Natural Resources, Municipal and Industrial Water Use Data, Accessed: 2021.

[34] California Department of Water Resources, Water Use Efficiency Data, Accessed: 2022.

[35] Illinois State Water Survey, Illinois Municipal Water Use, 2012, Accessed: 2021.

[36] Missouri Department of Natural Resources, Census of Missouri Public Water Systems, Accessed: 2021.

[37] New York State Department of Environmental Conservation, Water Withdrawal Data, Accessed: 2022.

[38] V. M. Savage, A. P. Allen, J. H. Brown, J. F. Gillooly, A. B. Herman, W. H. Woodruff, and G. B. West, Proc. Natl. Acad. Sci. USA **104**, 4718 (2007).

[39] R. De Veaux, P. F. Velleman, and D. E. Bock, *Intro Stats*, 6th ed. (Pearson, Hoboken, 2022).

[40] See Supplemental Material at http://link.aps.org/supplemental/10.1103/PhysRevE.107.034301 for dataplots and fits for the scaling parameters displayed in Fig. 1 and details of the insets in Fig. 4.

[41] S. Zaoli, A. Giometto, A. Maritan, and A. Rinaldo, Proc. Natl. Acad. Sci. USA **114**, 10672 (2017).

[42] L. M. A. Bettencourt, J. Lobo, D. Helbing, C. Kühnert, and G. B. West, Proc. Natl. Acad. Sci. USA **104**, 7301 (2007).

[43] J. R. Banavar, J. Damuth, A. Maritan, and A. Rinaldo, Proc. Natl. Acad. Sci. USA **99**, 10506 (2002).

[44] T. Nishikawa and A. E. Motter, Phys. Rev. Lett. **117**, 114101 (2016).

[45] M. Begon and C. R. Townsend, *Ecology: From Individuals to Ecosystems*, 5th ed. (Wiley, New York, 2021).

[46] J. Lobo, L. M. A. Bettencourt, D. Strumsky, and G. B. West, PLoS One **8**, e58407 (2013).

[47] C. Brelsford, J. Lobo, J. Hand, and L. M. A. Bettencourt, Proc. Natl. Acad. Sci. USA **114**, 8963 (2017).

[48] Utah Division of Water Resources, *Water Resources Plan*, Salt Lake City, UT, 2021.

[49] California Department of Water Resources, The California Water System, Accessed: 2022.

[50] F. Vasseur, M. Exposito-Alonso, O. J. Ayala-Garay, G. Wang, B. J. Enquist, D. Vile, C. Violle, and D. Weigel, Proc. Natl. Acad. Sci. USA **115**, 3416 (2018).

[51] E. R. Weibel, Nature (London) **417**, 131 (2002).

[52] C. R. White, Nature (London) **464**, 691 (2010).

[53] C. Cottineau, E. Hatna, E. Arcaute, and M. Batty, Comput. Environ. Urban Syst. **63**, 80 (2017).

[54] J. Jacobs, *The Death and Life of Great American Cities* (Random House, New York, 1961).

[55] C. Smith, *Plan of Chicago: Daniel Burnham and the Remaking of the American City* (University of Chicago Press, Chicago, 2006).

[56] P. Wiersma, A. Muñoz-Garcia, A. Walker, and J. B. Williams, Proc. Natl. Acad. Sci. USA **104**, 9340 (2007).

[57] P. Wiersma, B. Nowak, and J. B. Williams, J. Exp. Biol. **215**, 1662 (2012).

[58] IPCC, *Climate change and land: An IPCC special report on climate change, desertification, land degradation, sustainable land management, food security, and greenhouse gas fluxes in terrestrial ecosystems* (Intergovernmental Panel on Climate Change, Geneva, Switzerland, 2020).

[59] M. Burke, S. Hsiang, and E. Miguel, Nature (London) **527**, 235 (2015).